ELSEVIER

Thermochimica Acta 366 (2001) 47–59

thermochimica acta

www.elsevier.com/locate/tca

The formation of Cu_2S from the elements II. Copper used in form of foils

R. Blachnik*, A. Müller

Institut für Chemie, Universität Osnabrück, Barbarastraße 7, D-49069 Osnabrück, Germany

Received 22 May 2000; received in revised form 24 May 2000; accepted 5 September 2000

Dedicated to Prof. Dr. Hans-Joachim Seifert on the occasion of his 70th birthday.

Abstract

The synthesis of Cu_2S from copper foils embedded in sulfur has been studied by DTA from 25 to 600°C with a heating rate of 10 K/min. The educts and products were characterized by microscopic, microprobe and X-ray measurements.

Two main reactions take place: one immediately after melting of sulfur and the other above 300°C. During the first reaction a non-uniform layer containing CuS, $Cu_{1.1}S$, $Cu_{2-x}S$ with gaps is observed. Its copper content increases from outside to inside. After the first main effect the reaction stops due to a removal of the layer from the foil. Therefore, diffusion of copper vacancies is hindered. Starting with the second main effect, the reaction mechanism changes because $Cu_{2-x}S$ decomposes into copper and gaseous sulfur, which then reacts with the foil. This leads to a dense outside layer and a porous layer around the foil. Both consist of $Cu_{2-x}S$.

In direct contact with liquid or solid sulfur always CuS or $Cu_{1.1}S$ is formed whereas in contact with gaseous sulfur at first $Cu_{2-x}S$ appears.

After the reaction either a cavity surrounded by a dense layer or a dense layer on an inner porous layer are produced which probably depends on geometry and size of the copper sample.

Keywords: Copper; Sulfur; Copper sulfide; Solid state reaction; Reactivity

1. Introduction

In view of the lack of knowledge and of contradictory results on the reaction between copper and sulfur we investigated the factors which influence the formation of Cu_2S from the elements. In the first paper copper was used in form of powders [1]. Investigated parameters were amongst others: shape of samples (powders or pellets), mechanical treatment, pre-treatment, particle size, and aging. Now we have investigated the complete reaction of copper foils with liquid sulfur under dynamic conditions with DTA. Intermediate and final products were characterized by microscopic observations, X-ray and microprobe analyses.

Copper foils form in solutions of sulfur in organic solvents immediately dark layers of CuS or Cu_2S [2,3]. Copper foils turn black if rubbed with sulfur or stored with sulfur in an evacuated container without direct contact of the elements [4].

Some authors studied the reaction of copper foils, whiskers, wires, or single crystals with gaseous sulfur

* Corresponding author. Fax: +54-19693323.
E-mail address: bl@chnik.de (R. Blachnik).

0040-6031/01/$ – see front matter
PII: S0040-6031(00)00711-5

under isothermic conditions. Most investigations were performed at low-vapor pressures to obtain surface layers of copper sulfides [2,5–8]. Only in one case complete reaction was reported [9,10].

The structure of very thin epitaxial sulfide layers on single crystal films of copper did not depend on the substrate temperature but on exposure time or layer thickness, when the vapor pressure of sulfur is very low. The overgrowth started as $Cu_{2-x}S$ ($x = 0$) but transformed to β-Cu_2S and finally to α-Cu_2S with increasing thickness of the layer [7,8].

Tazaki and Kuwabara [5] worked at rather high-vapor pressures and found that at lower substrate temperatures a CuS layer and at higher temperatures a layer with more copper rich sulfides were produced.

Trehan and Goswami [6] observed on a single crystal face up to four different sulfide layers when the reaction rate was very slow. At first copper rich sulfides were formed and on further reaction the top layer consisted entirely of CuS. Higher reaction rates were obtained at higher vapor pressure and led to rough layers of CuS which often peeled off from the substrate. Polycrystalline copper reacted similarly but faster.

Lambertin and Colson [9,10] studied the sulfidation kinetics of thin copper wires and whiskers between 150 and 450°C and 1–130 Pa vapor pressure of sulfur. Below 310°C CuS and above this temperature digenite with the composition $Cu_{1.84}S$ were formed. The authors showed that cavity formation caused by metal consumption started at the metal/sulfide interface and grew inwards as the reaction proceeded. An exterior honeycombed region was observed which was traversed by metal bridges and filaments linking the internal metal core to the sulfide. The bridges assured the metal supply and disappeared when the conversion was completed. The reaction produced a thick, dense protecting sulfide layer. The rate of reaction was determined by the diffusion through this layer. In substrates with cylindrical or spherical symmetry a global strain can be produced at the internal metal/sulfide interface, which could cause a partial separation of the sulfide layer or even its rupture.

Recently, Tereshkova [11] studied scaling of copper rods with gaseous sulfur at 445°C. Two non-stoichiometric copper sulfide layers (digenite) were found, close in their chemical composition and different in their densities. The inner sulfide layer was porous and filled the space between the outer dense layer and copper. The growth of the two layers obeyed the parabolic law limited by copper ion diffusion.

2. Compounds and diffusion

In the first paper some information about the Cu–S phase diagram and metastable compounds were given [1].

The structures of the stable copper sulfides can be divided into three groups, which are based upon the packing of the sulfur anions. In the structures of α-Cu_2S, β-Cu_2S, and $Cu_{1.95}S$, the sulfur atoms are arranged in hexagonal close-packing and in the structures of $Cu_{2-x}S$ and $Cu_{1.75}S$ in cubic close-packing. In CuS and $Cu_{1.1}S$ hexagonal close-packing of sulfur is combined with covalent bonding between sulfur atoms [12]. While the high-temperature phases $Cu_{2-x}S$ and β-Cu_2S are highly disordered, the low-temperature phases α-Cu_2S, $Cu_{1.95}S$, and $Cu_{1.75}S$ form complex ordered superstructures. The high-ordering leads to a week distortion of the sulfur framework [13–16]. In all stable copper sulfides copper is monovalent [17,18].

Only copper participates in the bulk diffusion process in copper sulfides because the self-diffusion coefficient of sulfur is five to six orders of magnitude lower than that of copper [11,19]. The diffusion model based on negatively charged copper vacancies and electron holes which move in the same direction [10,20,21]. The chemical diffusion coefficients of copper within the homogeneity range of a phase are constant ($Cu_{1.95}S$) or decrease with increasing sulfur content (α-Cu_2S, $Cu_{2-x}S$) [20,22,23]. An Arrhenius-type of temperature dependence was found for the chemical diffusion coefficients of copper [24,25]. Less is known about diffusion phenomena in CuS.

3. Experimental

3.1. Methods

The characterization of samples with DTA, DSC, and X-ray measurements was previously described [1].

Microprobe analyses were performed with an electron beam X-ray microprobe SX 50 (Cameca). The samples were embedded in transparent resin, sanded, followed by further plastic mounting procedures to fill the internal cavities, polished and then sputtered with carbon.

Light microscopic pictures were taken with a special reflected-light microscope (Reichert) for micrographic determination with an option for polarized light.

Scanning electron microscope pictures were taken with a DMS 962 (Zeiss). Non-conductive samples were sputtered with gold.

3.2. Chemicals

Table 1 contains sources and some properties of copper and sulfur, used in the studies. Oxide layers on the surface of copper foils were removed with half concentrated HCl or by dipping the hot foil which was pre-heated in argon atmosphere into ethanol. Sulfur was recrystallized twice from CS_2 and treated in vacuum at 150°C for 0.5 h to remove solvent and traces of water. After purification the elements were stored under argon.

In all cases coarse ground sulfur and, if not otherwise mentioned, foils reduced in ethanol were used.

3.3. Preparation and measurement

Samples with the stoichiometry ($2Cu + S$) were obtained by weighing corresponding amounts of the elements (accuracy ± 1.0 mg) into quartz ampoules. These ampoules were heated in vacuum to remove water, flushed with argon, and then filled. During sealing the end of the ampoule was cooled to prevent reaction. Immediately after sealing the samples were used for thermal analyses to avoid aging effects. The arrangements of the educts are shown in Fig. 1. In DTA experiments approximately one half of the copper foils was embedded in the sulfur, therefore reactions had to be distinguished between those of copper in contact with liquid sulfur or with gaseous sulfur. In DSC experiments foils lay on sulfur.

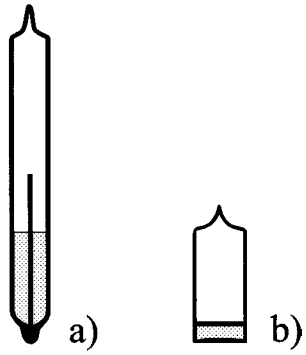

Fig. 1. Arrangement of samples. Copper foil: black; sulfur: grey. (a) DTA; (b) DSC.

Thermal effects were characterized with ex situ microprobe measurements by quenching samples from the temperatures of the peak onset, the maximum and the end of the effect in an ice-water mixture. In samples for microprobe analyses residual elemental sulfur was removed with CS_2. After the microprobe measurements, the samples were polished and light microscopic pictures were taken. Then the samples were measured with XRD.

Different reaction layers for X-ray measurements were separated by removing the inner layers with a dissecting needle. Most samples contained a mixture of copper rich sulfides after complete reaction, due to the slight excess of sulfur in the preparation.

To investigate the surface of partly reacted copper foils copper sulfides were dissolved in a solution of NaCN in water.

Table 1
Copper and sulfur used in this work

Element	Source	Shape	Purity[a] (%)	Purification methods
Copper	Goodfellow	Foil[b]	OFHC[c], 99.95	Reduced in ethanol or cleaned in HCl
Sulfur	Riedel	Powder	99.5	Recrystallized

[a] Given by producer, for copper only metallic impurities.
[b] ∅ 500 μm.
[c] Oxygen free high-conductivity.

In aging experiments one part of samples was stored in contact with sulfur, another one separated from sulfur in a sulfur atmosphere, both in evacuated quartz ampoules at room temperature.

The influence of heating rates was investigated using a DSC 404 (Netzsch) with heating rates of 0.5, 2.5, 10, and 40 K/min.

4. Results and discussion

4.1. Characterization of copper and sulfur

In the first paper as-received and purified sulfur and copper samples from various sources were characterized by DTA and XRD [1].

The typical melting peak of copper was observed with oxygen-free copper foils [1]. SEM pictures of the surface of a copper foil are shown in two magnifications in Fig. 2. No differences between as-received and cleaned copper foils were found. The thermoanalytical data of recrystallized sulfur agreed well with literature data cited in [1].

4.2. Reproducibility

Some experiments were repeated several times to ensure that differences in the reaction products and temperatures are due to alteration of parameters.

The samples were investigated under identical conditions to judge the influence of inaccuracy of weighing, differences in foil shape, and aging. Only the peaks and shoulders following the main reaction peak (F4, Fig. 3) were not reproducible with respect to onset temperature and number of effects. At higher temperatures large thermal effects also showed differences. The average standard deviations of reaction temperatures (phase transition temperatures) are $\pm 5.0^{\circ}C$ ($\pm 1.2^{\circ}C$). The reproducibility of thermal effects using foils embedded in sulfur is better than those of powders and pellets [1]. Different DTA traces are presented in Fig. 3. In Fig. 4 the standard deviations are given with respect to onset temperatures. The maximum is found at higher temperatures.

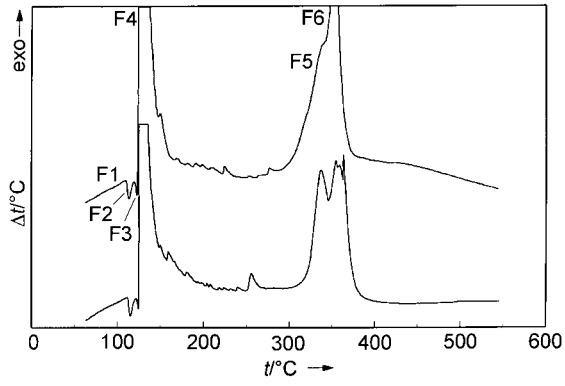

Fig. 3. DTA traces of different (2Cu + S) samples examined under identical conditions.

4.3. Analyses of DTA traces

The course of the reaction on heating (Table 2) can be described with the results of XRD investigations

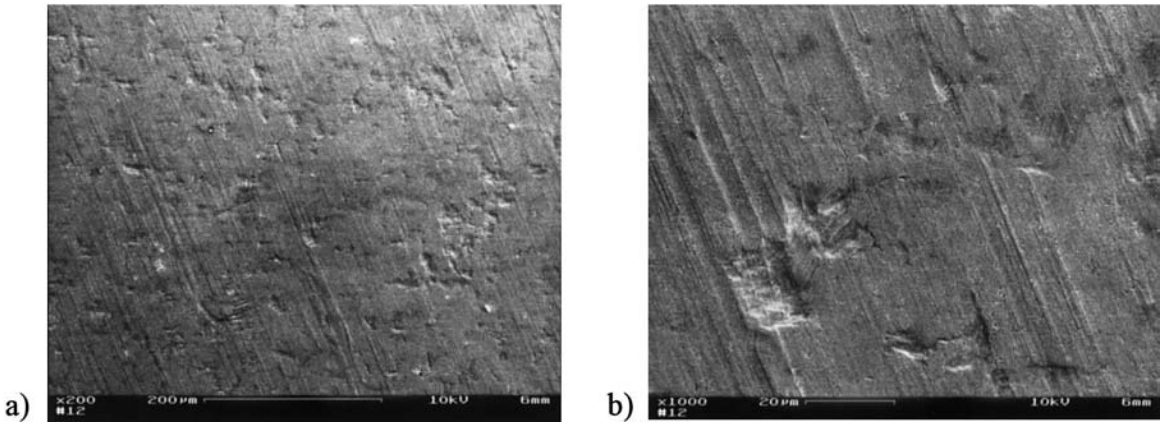

Fig. 2. SEM pictures of the surface of a copper foil as-received.

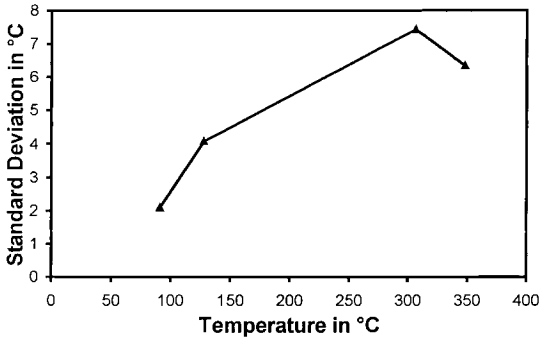

Fig. 4. Average values of the standard deviations of the onset temperatures of reactions.

(Table 3), of the microscopic observations and the microprobe measurements (Table 4). The hypothetic formulae which correspond to the molar fraction obtained by microprobe analyses are given in brackets. Notation of peaks can be taken from Fig. 3. Table 2 contains the peak onset temperatures. Sulfur rich $Cu_{2-x}S$ transformed after quenching into $Cu_{1.8}S$ and copper rich $Cu_{2-x}S$ into $Cu_{1.95}S$, $Cu_{1.96}S$, or α-Cu_2S, as detected by XRD (Table 3).

A weak exothermic effect (F1) was sometimes observed at ca. 91°C, usually it was hidden by the phase transformation of sulfur (F2). In our opinion the effect is caused by the formation of CuS on the surface. Melting of sulfur (F3) is only indicated, because it is superimposed by a strong exothermic reaction (F4). This reaction takes place on the foil in contact with liquid sulfur and produces on the outside layers with a copper content of $x_{Cu} = 0.53$ (“$Cu_{1.15}S$”) which are dyed blue by covellite, CuS (Fig. 5). The deviation from the ideal composition CuS has two reasons: the layers contain small amounts of $Cu_{2-x}S$ and of metastable yarrowite, $Cu_{1.1}S$ [26]. The latter was observed by Moh [27,28] in similar experiments. We did not detect this phase by XRD or microprobe analyses, but in microscopic experiments. CuS gets red with polarized light whereas yarrowite remains blue [28,29]. The occurrence of spionkopite, $Cu_{1.4}S$ [12,30], another metastable blue remaining covellite, was excluded by XRD measurements.

With increasing distance from the outside the digenite content increases which leads to copper contents in the range $x = 0.55$ (“$Cu_{1.3}S$”) to $x = 0.62$ (“$Cu_{1.6}S$”). In direct contact with the copper foil thin layers of pure grey $Cu_{2-x}S$ appear, separated from the other layers and forming a gap to the copper foil. Cracks, mostly parallel to the copper surface, were observed in the product layer, however, they do not separate different phases and are sometimes filled with $Cu_{2-x}S$ (sample lq2, Table 4).

Fig. 5 shows a layer and Fig. 6 the surface of such a partly reacted copper foil. Compared with the unreacted foil (Fig. 2) the surface is more rough and rippled, many cubical pits are observed.

On further heating F4 is slowly decaying and followed by several peaks (between 4 and 16) starting in the flank. Their onset temperatures are not reproducible. These effects decrease with increasing temperature and vanish at ca. 260°C. They can be due to either reactions between domains of CuS and $Cu_{2-x}S$ or fluctuations in the reaction rate caused by strain. The latter leads to sudden changes in the contact area of the copper/copper sulfide interface. The first hypothesis is supported by the observation that after these effects zones of different phases are better separated than immediately after the maximum of F4. The reason for bigger thermal effects which occur sometimes close to F4 may be large cracks in the sulfide layer which allow direct contacts of liquid sulfur with the copper foil.

After these effects the product consists on the outside of a thin layer with $x_{Cu} = 0.51$ (“$Cu_{1.05}S$”) and near to the copper foil of a thick layer of sulfur rich $Cu_{2-x}S$. These two layers can be separated by a thin region which contains both phases.

On the part of the foil in contact with gaseous sulfur only a very thin layer of grey sulfur rich $Cu_{2-x}S$ is

Table 2
Thermal effects as-detected by DTA of foils embedded in sulfur (2Cu + S)

	Effect					
	F1	F2	F3	F4	F5	F6
Type of reaction	Exothermic	Endothermic	Endothermic	Exothermic	Exothermic	Exothermic
Temperature (°C)	91 ± 2	107 ± 1	122 ± 1	128 ± 4	306 ± 7	348 ± 6

Table 3
Phases observed in quenched samples

Interruption of the reaction		Source of layers	Products[a]
During	F4		CuS [33], $Cu_{1.8}S$ [34]
After	F4	Layers which peeled off	CuS, $Cu_{1.8}S$
		Layers which sticked at the foil	$Cu_{1.8}S$, CuS, $Cu_{1.95}S$ [35]
Between	F4 and F5		$Cu_{1.8}S$, CuS
Before	F5[b]		$Cu_{1.8}S$, CuS
During	F6	Porous inner layers	$Cu_{1.8}S$, $Cu_{1.95}S$
		Dense outer layers	$Cu_{1.8}S$, $Cu_{1.95}S$
After	F6[b]		$Cu_{1.95}S$, $Cu_{1.8}S$, $Cu_{1.96}S$ [36][c]
After	F6	Porous inner layers	$Cu_{1.95}S$, $Cu_{1.8}S$, $Cu_{1.96}S$
		Dense outer layers	$Cu_{1.8}S$, $Cu_{1.95}S$, $Cu_{1.96}S$
After cooling		Porous inner layers	$Cu_{1.96}S$, $Cu_{1.95}S$
		Dense outer layers	$Cu_{1.96}S$, $Cu_{1.95}S$, α-Cu_2S [37]

[a] Phases in the order of intensities of XRD reflections.
[b] Foils previously cleaned in HCl.
[c] (↓) Very low-concentration.

formed up to 150°C, then the layer thickness increases rapidly. After ca. 200°C a thin CuS film is formed on the $Cu_{2-x}S$ layer which thickens in the course of the reaction. At the same time in the reaction zone with liquid sulfur the CuS content decreases so that the products in the two reaction zones differ mainly in the extent of conversion.

After the first main effect (F4) the reaction stops. With increasing removal of the reaction layer from the foil contacts by which copper can diffuse into the reaction zone are diminishing.

Differing intermediate products were not only observed vertical to the copper foil but also in regions parallel to the foil, as shown by Fig. 7, in which large

Table 4
Layers observed in quenched samples[a]

Interruption of the reaction		Molar fraction of copper[b]
During	F4	g: 0.63 ($Cu_{1.72}S$)/0.64 ($Cu_{1.80}S$), 1.00 (Cu)
		lq1: 0.53 ($Cu_{1.15}S$)/0.53 ($Cu_{1.12}S$)/0.54 ($Cu_{1.16}S$), 0.59 ($Cu_{1.47}S$), 0.56 ($Cu_{1.27}S$)/0.64 ($Cu_{1.79}S$)/1.00 (Cu)
		lq2: 0.53 ($Cu_{1.12}S$)/0.53 ($Cu_{1.11}S$)/0.64 ($Cu_{1.79}S$), 0.53 ($Cu_{1.11}S$), 0.57 ($Cu_{1.30}S$), 0.54 ($Cu_{1.17}S$), 0.65 ($Cu_{1.83}S$), 0.61 ($Cu_{1.58}S$), 0.64 ($Cu_{1.81}S$)/1.00 (Cu)
		lq3: 0.52 ($Cu_{1.09}S$), 0.56 ($Cu_{1.27}S$)/0.62 ($Cu_{1.64}S$)/1.00 (Cu)
After	F4	g: 0.60 ($Cu_{1.50}S$)/0.63 ($Cu_{1.68}S$)/0.61 ($Cu_{1.58}S$)/1.00 (Cu)
		lq: 0.51 ($Cu_{1.05}S$), 0.55 ($Cu_{1.23}S$), 0.51 ($Cu_{1.05}S$)/0.51 ($Cu_{1.05}S$), 0.61 ($Cu_{1.53}S$)/1.00 (Cu)
Between	F4 and F5[c]	g: 0.64 ($Cu_{1.77}S$)/1.00 (Cu)
		lq: 0.64 ($Cu_{1.77}S$)/0.64 ($Cu_{1.79}S$)/1.00 (Cu)
Before	F5[d]	g: 0.51 ($Cu_{1.04}S$)/0.62 ($Cu_{1.61}S$)/0.63 ($Cu_{1.73}S$)/0.64 ($Cu_{1.77}S$)/0.67 ($Cu_{2.00}S$), 1.00 (Cu)
		lq: 0.51 ($Cu_{1.03}S$)/0.51 ($Cu_{1.04}S$), 0.56 ($Cu_{1.27}S$)/0.63 ($Cu_{1.72}S$)/0.66 ($Cu_{1.92}S$), 1.00 (Cu)
After	F6[d]	g: dl 0.67 ($Cu_{2.02}S$)/pl 0.67–0.67 ($Cu_{2.07}S$–$Cu_{2.00}S$)/1.00 (Cu)
		lq: dl 0.66 ($Cu_{1.97}S$)/pl 0.67–0.66 ($Cu_{2.06}S$–$Cu_{1.94}S$)
After cooling		g: dl 0.66 ($Cu_{1.97}S$)/pl 0.66 ($Cu_{1.97}S$)
		lq: dl 0.67 ($Cu_{1.99}S$)/pl 0.67 ($Cu_{1.99}S$)

[a] lq: Copper foil in contact with liquid sulfur during reaction; g: copper foil in contact with gaseous sulfur during reaction; /: gap between the layers; dl: dense layer; pl: porous layer.
[b] From outside to inside, formulae of the corresponding hypothetic composition given in brackets.
[c] Without the outside layers.
[d] Foils previously cleaned in HCl.

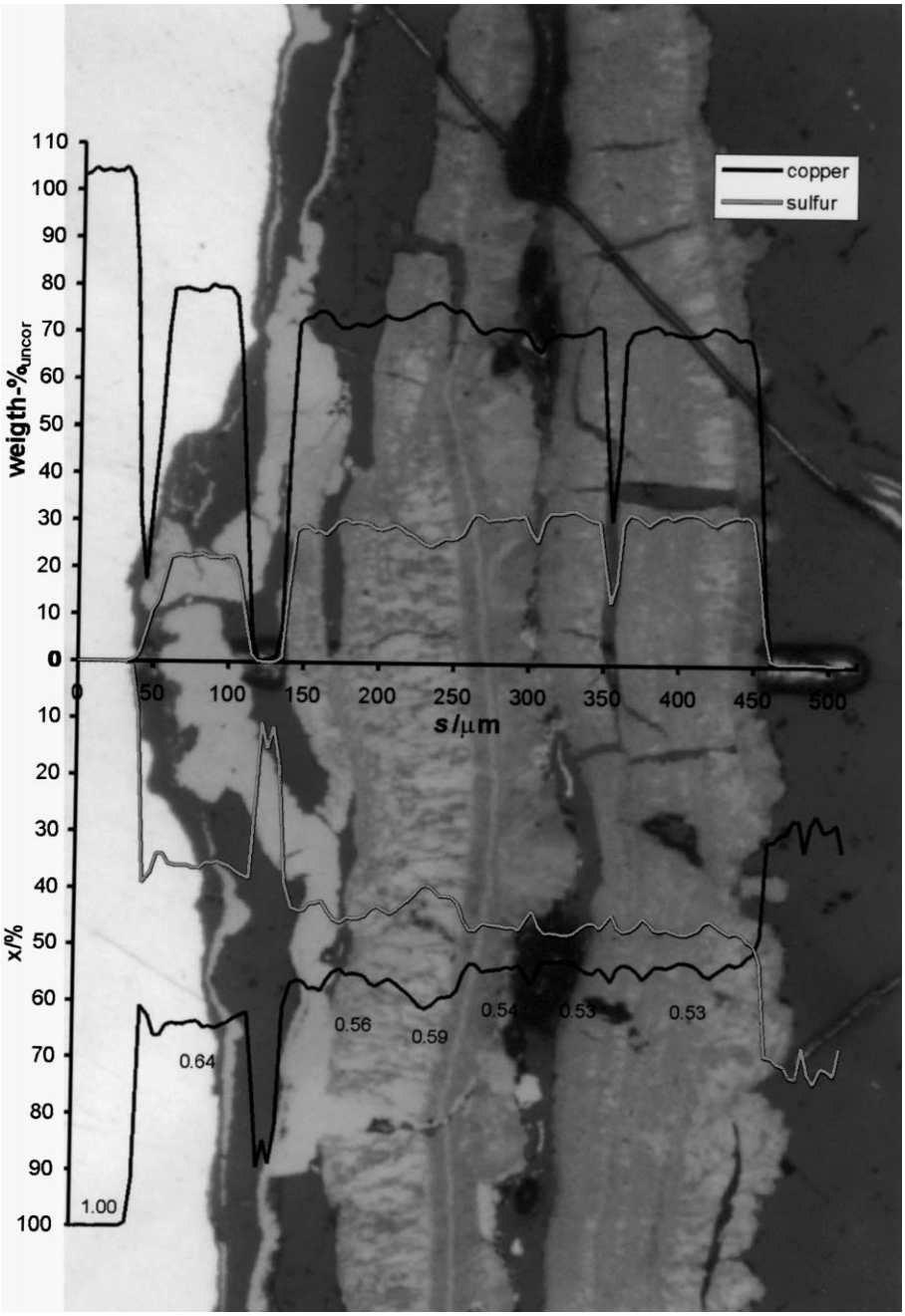

Fig. 5. Micrograph of a partly reacted (2Cu + S) sample (quenched during F4, in contact with liquid sulfur) combined with the corresponding results of a microprobe scan. White region: Cu foil; grey regions: CuS, $Cu_{1.1}S$; light grey regions: $Cu_{1.8}S$; dark grey regions: hardened resin; black regions: holes in the hardened resin. The trace of the electron beam of the microprobe is visible in the hardened resin and is placed under the *s*-axis of the diagram. The values in *s*–*x* diagram are the mole fraction of copper of the corresponding region (sample 1q1, Table 1).

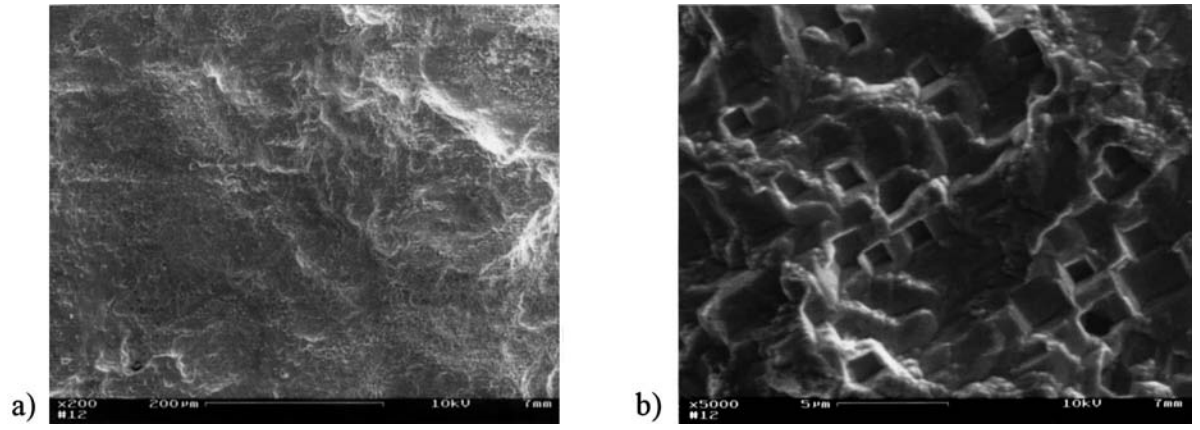

Fig. 6. SEM pictures of the surface of the product free copper foil of Fig. 5.

globes of $Cu_{2-x}S$ are linked by CuS bridges. A comparison of the boundary of the foil with the position of the products reveals that copper stems from the foil directly underneath the product thus minimizing the diffusion path.

On further heating, a strong exothermic effect (F6) appears at ca. 348°C, occasionally with a shoulder (F5) at ca. 306°C. All elemental sulfur and CuS have reacted to $Cu_{2-x}S$ when the maximum of F6 is reached. The layer is now grey.

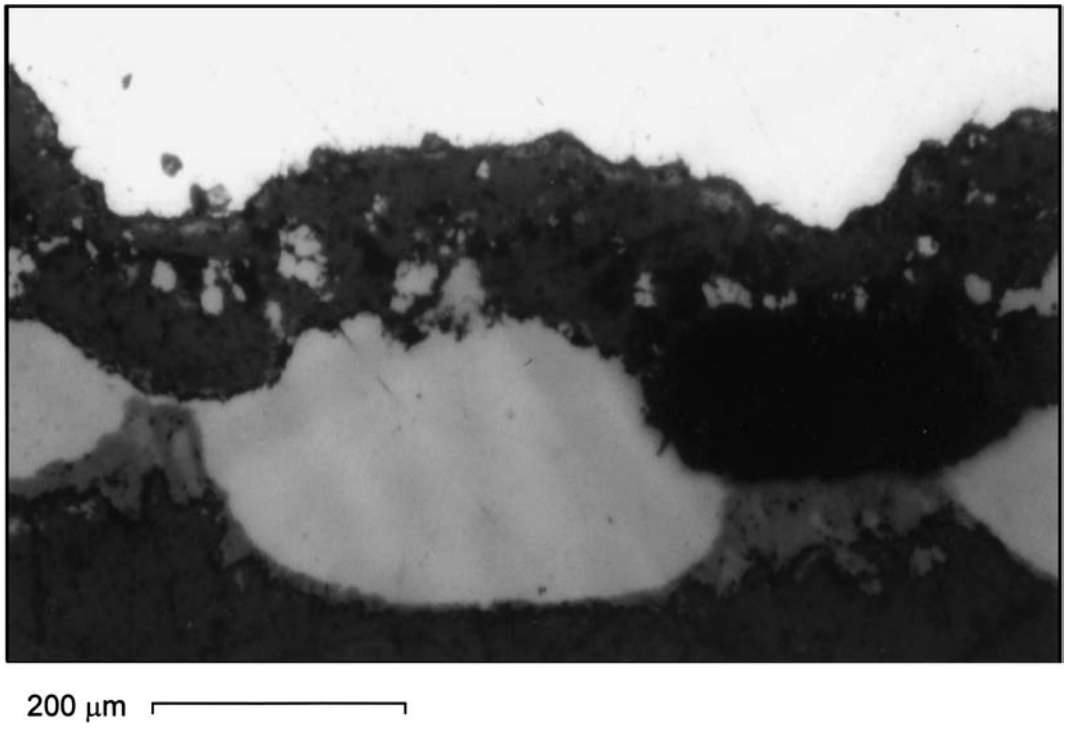

Fig. 7. Micrograph of a partly reacted (2Cu + S) sample (quenched before F5, in contact with gaseous sulfur). White regions: Cu foil; light grey regions: $Cu_{1.8}S$; grey region (between and at the border of light grey regions): CuS; dark grey regions: hardened resin; black regions: holes in the hardened resin.

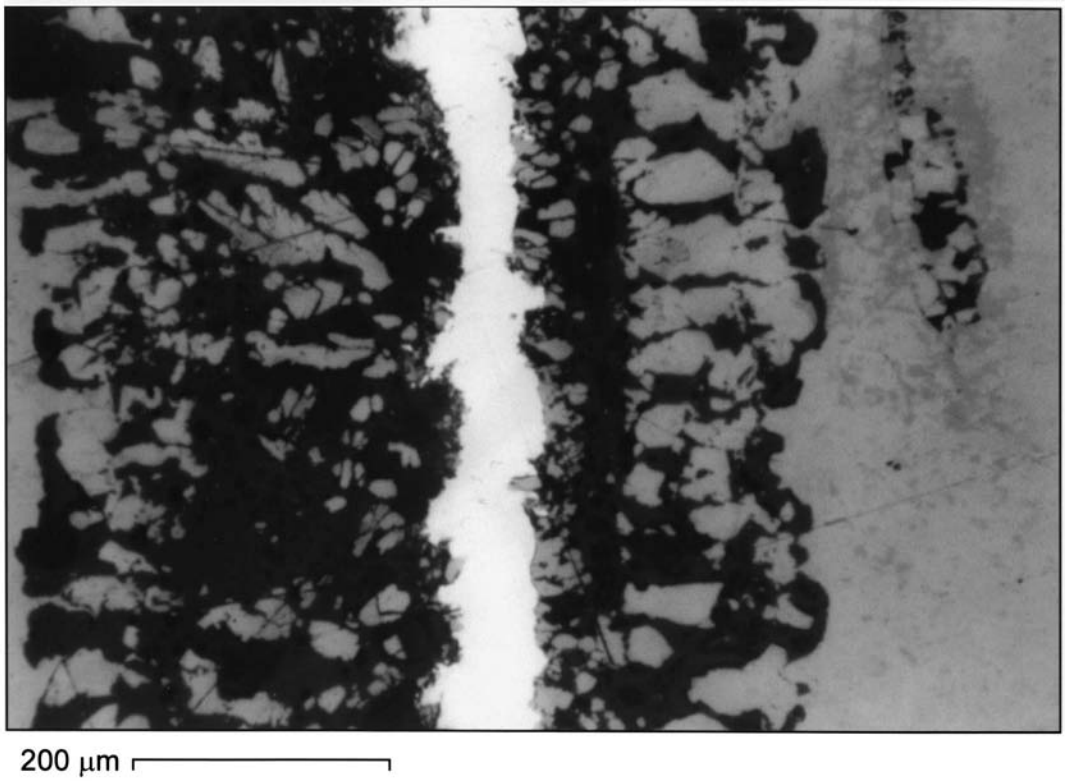

Fig. 8. Micrograph of a partly reacted (2Cu + S) sample (quenched after F6, in contact with gaseous sulfur). White region: Cu foil; light grey regions: $Cu_{1.95}S$, $Cu_{1.8}S$, $Cu_{1.96}S$; dark grey regions: hardened resin; black regions: holes in the hardened resin.

Starting with this second main effect the reaction mechanism and morphology in the layer changes in the manner described by Tereshkova [11]. On the outside a dense zone without cracks is formed. The layer next to the foil is porous with no mechanical stability (Fig. 8). The dense layer of $Cu_{2-x}S$ partly decomposes into copper and sulfur forming the inner porous layer. Copper can diffuse to the outside, gaseous sulfur can react with the copper foil. This mechanism was first described by Dravnieks and McDonald [31]. If one neglects the residual contacts in the copper/copper sulfide interface the situation is that of copper sulfide in a strong sulfur potential gradient. With these conditions oxides are reduced at the side with low-oxygen potential which lead to morphological unstable surfaces [32].

The copper content of both layers is nearly identical. The boundary of the foil is now strongly fissured during the reaction. After F6 the rests of the foil vanish on further heating. The last position of the foil is revealed by a dense arrangement of copper sulfide particles (backbone marked in Fig. 9).

Samples which are heated to 550°C and cooled slowly contain a mixture of α-Cu_2S, $Cu_{1.96}S$, and $Cu_{1.95}S$. We found after the reaction small longish cavities of different sizes bordered by porous layers. These porous layers were copper sulfide crystals which sticked inside the outer dense layer. We conclude that with sufficient annealing times and temperatures the porous layer is consumed. Thus the surface energy minimizes and cavities with comparable volume to that of the consumed metal may be formed.

Contrary to the report of Lambertin and Colson [9,10] we neither observed bridges of copper, which allow continuous diffusion, nor cavities corresponding to the volume of the metal at the end of the reaction. In reaction mixtures with copper powders [1] with

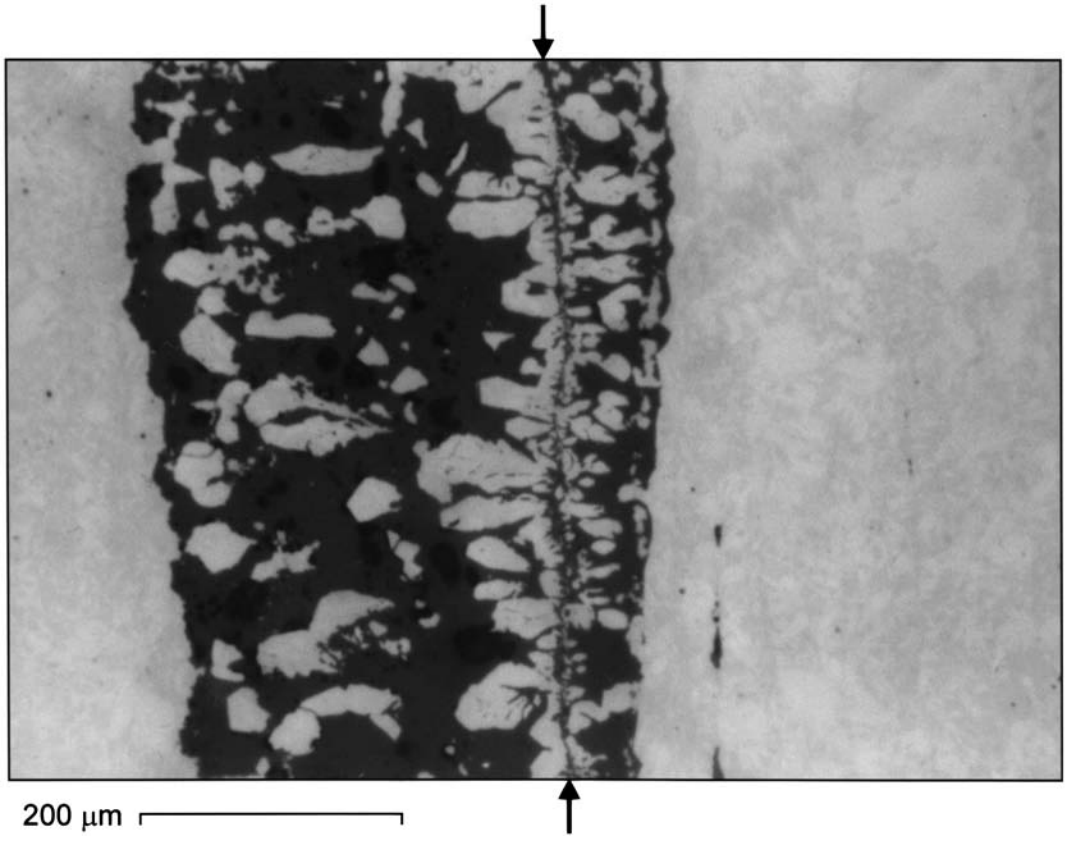

Fig. 9. Micrograph of a partly reacted (2Cu + S) sample (quenched after F6, in contact with liquid sulfur). Light grey regions: $Cu_{1.95}S$, $Cu_{1.8}S$, $Cu_{1.96}S$; dark grey regions: hardened resin; black regions: holes in the hardened resin. Arrows mark the last position of the vanished foil.

particle diameters in the range 36–100 μm, thus comparable with the diameter of copper wires (140 μm) or whiskers (50 μm) used by Lambertin and Colson, we never found porous layers but dense regions around cavities. Fig. 10 depicts a residual copper particle in such a cavity with almost the same appearance as observed by Colson and Lambertin [9, Fig. 8]. It seems that copper bridges from the inner particle to the dense layer occur (Fig. 10a) and copper fingers create a very large surface of the particle (Fig. 10b).

The copper/copper sulfide interface seems to be morphologically unstable in most cases at least at the end of the reaction. The unstability can affect copper or copper sulfide, depending on shape and size of the copper educt.

From the known facts reported in the introduction and our results it is evident that covellites are formed with high-sulfur concentrations and at low-temperatures. Copper rich sulfides are observed with low-sulfur vapor pressure or at high-temperatures. Therefore, Tereshkova [11] did not observe CuS (decomposition temperature 507°C) at 445°C even with a sulfur vapor pressure of 0.1 MPa. This effect is surprising under equilibrium conditions as given by Ellingham diagrams.

Fig. 11 depicts DTA traces of all forms of educts: powders reacted mainly after melting of sulfur. Pellets give DTA traces with overlapping effects, the biggest effects appearing at higher temperatures. DTA traces of foils embedded in sulfur possess two well separated main effects, one after the melting of sulfur and the other at higher temperature than that in case of the pellets. The part of reaction before the melting of sulfur decreases in the order powder, pellet, foil. In

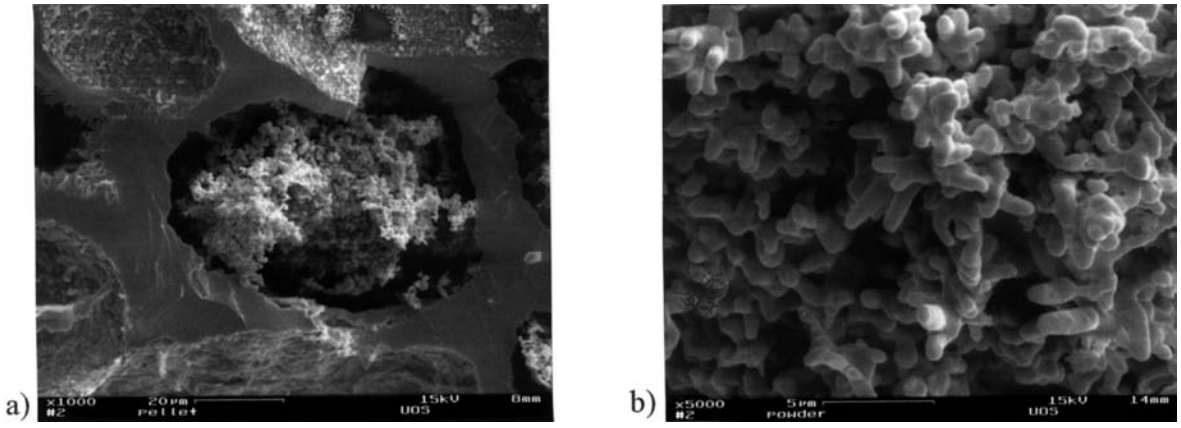

Fig. 10. SEM picture of a (2Cu + S) mixture with copper in the form of powders (heated to 550°C and then slowly cooled). (a) Residual copper particle in a cavity of a pellet sample; (b) magnification of such a particle of a powder sample.

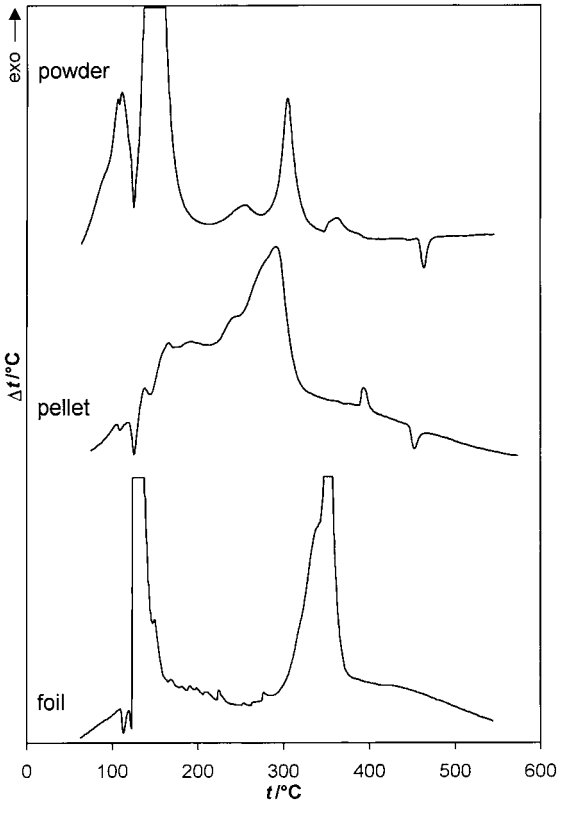

Fig. 11. Typical DTA traces of mixtures (2Cu + S) of samples in the form of powders [1], pellets [1], and foils embedded in sulfur.

spite of the different possible contact surfaces in powders ($A_s = 100\ cm^2/g$, average particle diameter $d = 70\ \mu m$ is assumed) and foils embedded in sulfur ($A_s = 3\ cm^2/g$) the first main reaction peaks are comparable. The end of the last main reaction peaks shifts for foils approximately 65°C to higher temperatures compared with those in pellets or powders. The overlap of the formation of intermediate products increases in the order powder, pellet, foil.

From the results with foils it is obvious that the reaction starts with the formation of CuS and $Cu_{1.1}S$ also in copper powders. However, its microscopic detection was not possible because the particle size was to small.

Compared with the DTA traces of educts in the form of powders or pellets generally the phase transition β-$Cu_2S \rightarrow Cu_{2-x}S$ ($x = 0$) (ca. 450°C) was not observed, because the composition of Cu_2S could not be reached due to the slight excess of sulfur used in the weighing procedure.

4.4. Influence of mechanical treatment and pretreatment

Mechanical treatment was achieved by rubbing the foil with sulfur powder until black layers appeared. The use of such foils in syntheses led within the reproducibility to similar DTA traces as with untreated

foils. Surprisingly, these layers have no protecting function, contradictory to observations of the reaction behavior when powders are used [1].

Foils reduced in ethanol or cleaned in HCl differ in their reaction behavior only in one point, after melting of sulfur the reaction starts somewhat faster on foils cleaned with HCl.

4.5. Influence of aging

One foil was placed in a sulfur atmosphere and stored for 10 months at room temperature. A second foil was embedded in sulfur and stored 86 days also at room temperature. The first darkened within hours and turned slowly to grey after several days. A microprobe measurement revealed a thin layer sticking at the foil with a molar fraction of copper of $x_{Cu} = 0.66$ (''$Cu_{1.92}S$''), probably by the formation of copper rich sulfides like low-digenite $Cu_{1.8}S$ or djurleite $Cu_{1.95}S$.

The second foil was colored deep blue which is typical for CuS. During the reaction small fibers peeled off. The product layers consisted of connected domes similar in height. A cross-section of the layer structure is depicted in Fig. 12. The distance between layer and foil was approximately eight times larger than the thickness of the layer. Microprobe and microscopic investigations showed that the domes consist of CuS and $Cu_{1.1}S$.

These results confirm the assumptions on the conditions for the formation of copper sulfides in Section 4.3.

4.6. Influence of the heating rate

The heating rate is a decisive factor for the reaction behavior. DSC traces of samples were taken with foils cleaned in HCl. For better comparison the heat flow ϕ was divided by the mass of the sample and the average heating rate β. Fig. 13 reveals that two main effects were observed. The onset temperature of the first reaction did not depend on the heating rate, but the onset of the second peak shifts from 207°C (0.5 K/min) to 414°C (40 K/min). The amount of products formed after melting of sulfur decreases from 79% at 0.5 K/min to 28% at 40 K/min. This behavior is opposite to that of pellets [1]. At slow heating rates the reaction starts before the melting of sulfur is indicated. Unlike to the reaction behavior in pellets [1] effect F1 (not visible in Fig. 13) does not increase with decreasing heating rates.

The very small endothermic effect at 437°C (0.5 K/min) is due to the phase transition β-$Cu_2S \rightarrow Cu_{2-x}S$ ($x = 0$).

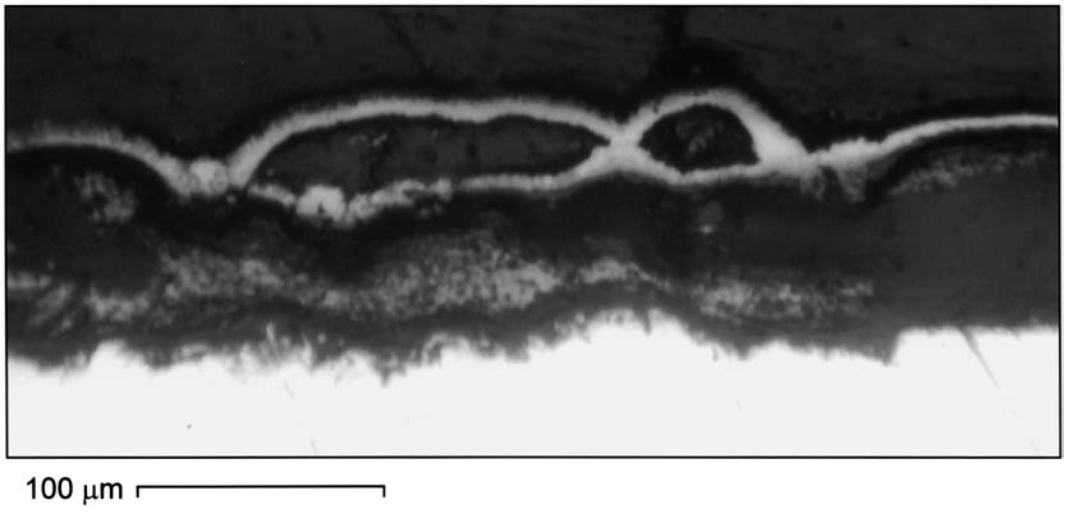

Fig. 12. Micrograph of a partly reacted copper foil which had been embedded 86 days in sulfur. White region at the bottom: Cu foil; white or light grey bows or rings: CuS, $Cu_{1.1}S$; all other parts of the picture: hardened resin.

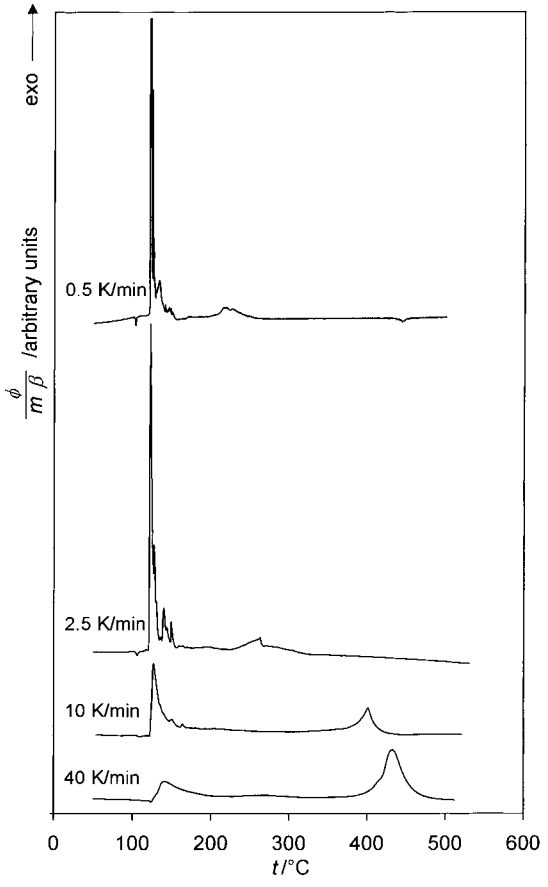

Fig. 13. DSC traces of foils embedded in sulfur of (2Cu + S) samples measured with different heating rates. Three quarters of the main peak of the trace with 0.5 K/min are cut off.

Acknowledgements

The authors express their gratitude to the ''Deutsche Forschungsgemeinschaft'' and the ''Fonds der Chemie'' for their support. Dr. Bernd Gather is thanked for the microprobe measurements and Dr. Ratheesh Ravendran and Mrs. Katharina Mey for their help in taking SEM pictures.

References

[1] R. Blachnik, A. Müller, Thermochim. Acta 361 (2000) 31.
[2] K. Fischbeck, Z. Anorg. Chem. 154 (1926) 261.
[3] Gmelins Handbuch der Anorganischen Chemie, 8th Edition, Vol. Cu Main B1, Verlag Chemie, Weinheim, 1958, p. 471.
[4] Gmelins Handbuch der Anorganischen Chemie, 8th Edition, Vol. Cu Main B1, Verlag Chemie, Weinheim, 1958, pages 435, 443.
[5] H. Tazaki, S. Kuwabara, J. Sci. Hiroshima Univ. A 14 (1950) 251.
[6] Y.N. Trehan, A. Goswami, Trans. Faraday Soc. 55 (1959) 2162.
[7] O.J. Cain, R.W. Vook, Thin Solid Films 51 (1978) 373.
[8] O.J. Cain, R.W. Vook, Thin Solid Films 58 (1979) 209.
[9] J.-C. Colson, M. Lambertin, P. Barret, React. solids, Proc. Int. Symp. 7 (1972) 283.
[10] M. Lambertin, J.-C. Colson, Oxid. Metals 7 (1973) 163.
[11] S.G. Tereshkova, Kinet. Catal. 39 (1998) 217.
[12] R.J. Goble, Can. Miner. 23 (1985) 61.
[13] H.T. Evans Jr., Z. Kristallogr. 150 (1979) 299.
[14] R.J. Cava, F. Reidinger, B.J. Wuensch, Solid State Ionics 5 (1981) 501.
[15] H.T. Evans Jr., Am. Miner. 66 (1981) 807.
[16] K. Yamamoto, S. Kashida, J. Solid State Chem. 93 (1991) 202.
[17] G. van der Laan, R.A.D. Pattrick, C.M.B. Henderson, D.J. Vaughan, J. Phys. Chem. Solids 53 (1992) 1185.
[18] J.C.W. Folmer, F. Jellinek, J. Less-Common Met. 76 (1980) 153.
[19] F. Moya, G.E. Moya-Gontier, F. Cabane-Brouty, J. Oudar, Acta Metall. 19 (1971) 1189.
[20] S. Cassaignon, T. Pauporte, J.-F. Guillemoles, J. Vedel, Ionics 4 (1998) 364.
[21] L.H. Allen, E. Buhks, J. Appl. Phys. 56 (1984) 327.
[22] V.N. Konev, V.N. Chebotin, S.A. Fomenkov, Inorg. Mater. 21 (1985) 166.
[23] U. Tinter, H.-D. Wiemhöfer, Solid State Ionics 9–10 (1983) 1213.
[24] T. Pauporte, J. Vedel, Solid State Ionics 116 (1999) 311.
[25] A. Etienne, J. Electrochem. Soc. 117 (1970) 870.
[26] PDF-2 Database, File 36-0379, International Centre for Diffraction Data, PA, USA, 1996.
[27] G.H. Moh, Carnegie Inst. Washington Year Book 1962 (1963) 214.
[28] G.H. Moh, Miner. Soc. Jpn. Spec. Pap. 1 (1971) 226.
[29] G. Frenzel, Neues Jb. Miner. 93 (1959) 87.
[30] PDF-2 Database, File 36-0380, International Centre for Diffraction Data, PA, USA, 1996.
[31] A. Dravnieks, H.J. McDonald, Trans. Electrochem. Soc. 94 (1948) 139.
[32] M. Martin, P. Tiegelmann, S. Schimschal-Thölke, G. Schulz, Solid State Ionics 75 (1995) 219.
[33] PDF-2 Database, File 06-0464, International Centre for Diffraction Data, PA, USA, 1996.
[34] PDF-2 Database, File 23-0962, International Centre for Diffraction Data, PA, USA, 1996.
[35] Inorganic Crystal Structure Database, Release 98/2, File 100334, FIZ Karlsruhe, Gmelin Institute, 1998.
[36] PDF-2 Database, File 29-0578, International Centre for Diffraction Data, PA, USA, 1996.
[37] Inorganic Crystal Structure Database, Release 98/2, File 100333, FIZ Karlsruhe, Gmelin Institute, 1998.